Springer

Journal of Mechanical Science and Technology 23 (2009) 901~909

Journal of
Mechanical
Science and
Technology

www.springerlink.com/content/1738-494x
DOI 10.1007/s12206-009-0309-4

Energy-consistent integration of multibody systems with friction †

Stefan Uhlar and Peter Betsch*

Chair of Computaional Mechanics, Department of Mechanical Engineering, University of Siegen, Paul-Bonatz-Str. 9-11, 57068 Siegen, Germany

(Manuscript Received December 24, 2008; Revised March 16, 2009; Accepted March 16, 2009)

Abstract

The main goal of the present contribution is to establish an energy consistent time integration procedure for multibody systems with friction. Based upon a rotationless formulation for multibody systems, we use the coordinate augmentation technique in order to implement frictional phenomena such as joint friction. Within this contribution we use the viscous friction assumption as a classical friction model incorporated in the joints. We start with a classical ad hoc model for damping and extend the formulation to multibody systems, dealing finally with an underactuated control problem of a three bar linkage with applied joint friction.

Keywords: Differential algebraic equations; Dissipation; Friction; Multibody system

1. Introduction

We use a rotationless formulation for multibody systems which has been shown to be especially well-suited for the design of energy-momentum conserving integration schemes [1, 2]. Energy-momentum schemes facilitate a stable numerical integration of differential algebraic equations (DAEs) with index three. The rotationless formulation of rigid bodies relies on redundant coordinates which coincide with the components of the rotation matrix. The constraint of rigidity is explicitly enforced by means of six independent constraints for enforcing the orthonormality of a body fixed director frame. The underlying DAEs facilitate the incorporation of additional 'external' constraints which account for the interconnection of rigid bodies in a multibody framework.

Although the rotationless formulation does not use rotational parameters, rotations are often required to model specific multibody systems. For example, joint-angles, associated joint-torques or joint friction are common modeling features. To incorporate rotations into our rotationless formulation we have previously developed in [3, 8] a coordinate augmentation technique. This approach represents an extension of the original rotationless formulation and thus preserves all the advantageous algorithmic conservations properties of the original scheme. In particular, for conservative multibody systems with symmetry, the time-stepping scheme inherits conservation of both the momentum maps (linear and angular momentum) and the total energy from the underlying continuous system.

Of course, friction effects play a major role for real world applications. Our goal is to develop an energy consistent integration method for nonconservative multibody systems. In particular, in the limit case of vanishing friction the original conserving method should be recovered. An energy consistent method should capture the dissipative properties correctly, independent of the time step. Standard integrators do not possess this property in general; see [5]. In the present work we will focus on the incorporation of joint-friction by making use of the aforementioned

† This paper was presented at the 4th Asian Conference on Multibody Dynamics(ACMD2008), Jeju, Korea, August 20-23, 2008.

*Corresponding author. Tel.: +49 271 740 2224, Fax.: +49 271 740 2241
E-mail address: betsch@imr.mb.uni-siegen.de

coordinate augmentation technique.

The outline of the current contribution is as follows. First (Section 2) we give a brief introduction to dissipative systems by a 1D model problem, dealing with a damped spring mass oscillator. Here we will define some important values and show how to check energetic consistency. In section 3 we give a short survey of the description of rigid bodies and the underlying equations of motion. An extension for nonconservative systems follows, accompanied with the example of a physical pendulum (Section 4.1). An extension to multibody systems is given in Section 4.2, by the incorporation of frictional effects, dealing finally with an underactuated control problem, where we will show how important friction phenomena for control problems are. The contribution ends with the conclusions.

2. 1D model problem

A first approach of how to handle dissipation is to consider a simple spring mass oscillator with a velocity dependent viscous damper, as visible in Fig. 1.

The equation of motion for this one DOF system yields to:

$$m\ddot{q} + d\dot{q} + cq = 0 \tag{1}$$

As one can see, the damping term is velocity dependent, representing a viscous damping element. This is in contrast to other damping models; see e.g. [9]. In the first instance we apply the second order accurate mid-point evaluation to perform a time integration of the equations above:

$$q_{n+1} - q_n = \Delta t\, v_{n+1/2} \tag{2}$$

$$m\left(v_{n+1} - v_n\right) + \Delta t\, d\, v_{n+1/2} + \Delta t\, d\, q_{n+1/2} = 0 \tag{3}$$

with

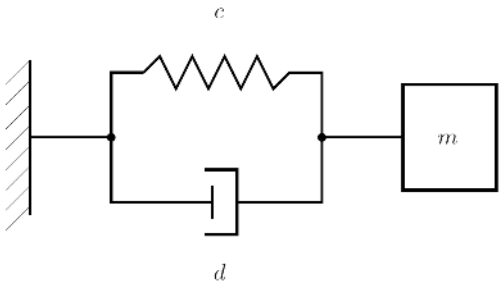

Fig. 1. Ad hoc model for friction (Kelvin-Voigt).

$$v_{n+1} = \frac{2}{\Delta t}\left(q_{n+1} - q_n\right) - v_n \tag{4}$$

A discrete version in terms of the configuration can be expressed as

$$\frac{2m}{\Delta t}\left(q_{n+1} - q_n\right) - 2mv_n + d\left(q_{n+1} - q_n\right) + \Delta t\, q_{n+1/2} = 0 \tag{5}$$

For non-conservative systems the following relationships can be stated

$$\begin{aligned} H &= -\mathcal{D} \\ \int H \,\mathrm{d}t &= -\int \mathcal{D} \,\mathrm{d}t \\ H_{n+1} - H_n + \Delta D &= R \end{aligned} \tag{6}$$

where the dissipation $\mathcal{D} \geq 0$ for all times t. Here H is the Hamiltonian concerning the conservative part, while R represents the residual equation which must be fulfilled for all times. The dissipation can be derived here as follows. Multiplying (1) with $\dot{q}$

$$m\ddot{q}\dot{q} + d\dot{q}\dot{q} + cq\dot{q} = 0 \tag{7}$$

performing a time integration

$$\int m\ddot{q}\dot{q}\,\mathrm{d}t + \int d\dot{q}\dot{q}\,\mathrm{d}t + \int cq\dot{q}\,\mathrm{d}t = \mathcal{H} \tag{8}$$

$$\underbrace{\int m\dot{q}\frac{\mathrm{d}\dot{q}}{\mathrm{d}t}\,\mathrm{d}t}_{T} + \underbrace{\int d\dot{q}\dot{q}\,\mathrm{d}t}_{\mathcal{A}_D} + \underbrace{\int c\,q\frac{\mathrm{d}q}{\mathrm{d}t}\mathrm{d}t}_{U} = \mathcal{H} \tag{9}$$

leading to the equivalence

$$\mathcal{H} = H + \mathcal{A}_D \tag{10}$$

Here $\mathcal{H}$ is the augmented Hamiltonian, consisting of the conservative part H and the non-conservative part $\mathcal{A}_D$. Where $\mathcal{A}_D$ stands for the accumulated dissipation, which can also be written as

$$\mathcal{A}_D = \int \mathcal{D}\,\mathrm{d}t \tag{11}$$

Energy consistency requires $\mathcal{D} \geq 0$ leading to a monotonic decrease of $\dot{H}$. In this first ad hoc approach, where we modelled a simple spring mass damper, with a linear damping characteristic, we can calculate the accumulated dissipation using the stan-

dard mid-point evaluation:

$$\mathscr{A}_D = \int d\,\dot{q}\,\dot{q}\,\mathrm{d}t \tag{12}$$

$$\mathscr{A}_D{}^{n+1} = \mathscr{A}_D{}^{n} + \Delta t\, d\,\dot{q}^2{}_{n+1/2} \tag{13}$$

Since the terms inside the time integral are at max. quadratic, the dissipation is calculated without any numerical errors.

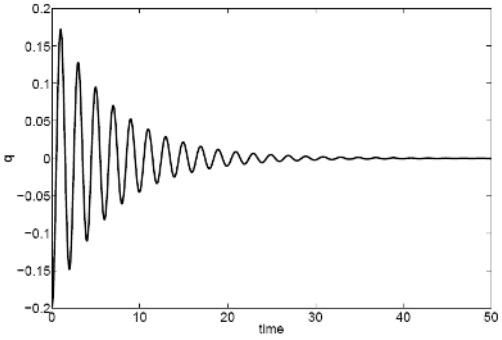

Fig. 2. displacement q.

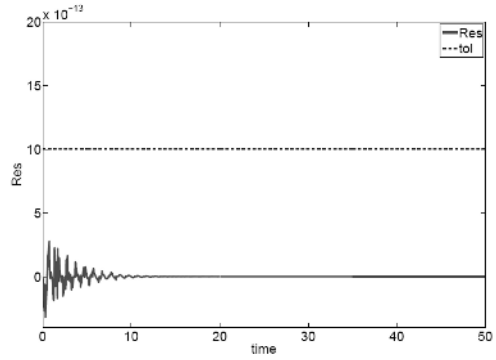

Fig. 3. Fulfillment of the residual.

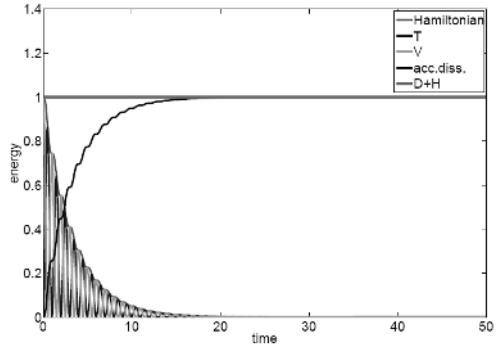

Fig. 4. Energy components for spring mass system.

2.1 Numerical example

Here we will present the results from the ad hoc model above. We choose a mass of $m = 5$, a spring stiffness of $c = 50$ and a viscous damping coefficient of $d = 1.5$; the time step size is $\Delta t = 0.05$. Fig. 2 shows the displacement q of the mass, as obvious the system is undercritically damped. To prove the consistency of our integrator presented above energetic consistency we check the residual equation $(6)_3$ which must be zero for all times (Fig. 3). Finally, the energy components are plotted in Fig. 4, split into the components of kinetic, potential and their sum, the Hamiltonian. The sum of the accumulated dissipation and the Hamiltonian renders a straight line which means that we obtained a consistent time integrator for the ad hoc dissipative model.

In the following we will adapt the procedure for multibody systems, where we will model joint friction using the same friction model as presented before.

3. Multibody systems

In this section we briefly describe rigid bodies and whole systems governed by a system of differential algebraic equations which arise due to the kinematic assumptions and external constraints combining rigid bodies. These formulations go back to works [1, 2]. The main focus is now on the incorporation of joint friction to these models. This can be facilitated by the coordinate augmentation technique, which was presented in [3, 8]. First we will present the basic equations of motion followed by the kinematics of a spatial rigid body. The incorporation of friction will be addressed and representative examples will follow.

3.1 Governing equations of the rotationless formulation

In this section we outline the equations of motion which provide a uniform framework for the rotationless formulation of multibody dynamics. For simplicity, we focus first here on discrete mechanical systems which are holonomic and scleronomic[1]. Accordingly, the equations of motion assume the form

[1] the extension to rheonomic systems will be given in Section 4.2.1

$$\begin{aligned} \dot{\mathbf{q}} - \mathbf{v} &= \mathbf{0} \\ \mathbf{M}\mathbf{v} - \mathbf{f}(\mathbf{q}) + \mathbf{G}^T(\mathbf{q})\boldsymbol{\lambda} &= \mathbf{0} \\ \boldsymbol{\Phi}(\mathbf{q}) &= \mathbf{0} \end{aligned} \tag{14}$$

Here, $\mathbf{q}(t) \in \Re^n$ specifies the configuration of the mechanical system at time *t*, and $\mathbf{v}(t) \in \Re^n$ is the velocity vector. Together $(\mathbf{q}, \mathbf{v})$ form the vector of state space coordinates (see, for example, Rosenberg [7]). A superposed dot denotes differentiation with respect to time and $\mathbf{M} \in \Re^{n \times n}$ is *constant* and symmetric mass matrix, so that the kinetic energy can be written as

$$T(\mathbf{v}) = \frac{1}{2}\mathbf{v} \cdot \mathbf{M}\,\mathbf{v} \tag{15}$$

Moreover, $\mathbf{f} \in \Re^n$ is a load vector which may be decomposed according to

$$\mathbf{f} = \mathbf{Q} - \nabla V(\mathbf{q}) \tag{16}$$

Here, $V(\mathbf{q}) \in \Re$ is a potential energy function and $\mathbf{Q} \in \Re^n$ accounts for loads which cannot be derived from a potential. Moreover, $\boldsymbol{\Phi}(\mathbf{q}) \in \Re^m$ is a vector of geometric constraint functions, $\mathbf{G} = D(\mathbf{q}) \in \Re^{m \times n}$ is the constraint Jacobian and $\boldsymbol{\lambda} \in \Re^m$ is a vector of multipliers which specify the relative magnitude of the constraint forces. In the above description it is tacitly assumed that the *m* constraints are independent.

Due to the presence of holonomic (or geometric) constraints $(14)_3$, the configuration space of the system is given by

$$\mathbf{Q} = \left\{ \mathbf{q}(t) \in \Re^n \,\middle|\, \boldsymbol{\Phi}(\mathbf{q}) = \mathbf{0} \right\} \tag{17}$$

The equations of motion (14) form a set of index-3 differential-algebraic equations (DAEs) (see, for example, Kunkel & Mehrmann [6]). They can be directly derived from the classical Lagrange's equations.

3.2 Discretization of the DAEs

For the discretization of the DAEs (14), we apply a specific approach which yields an energy-momentum conserving scheme. Consider a representative time interval $[t_n, t_{n+1}]$ with time step $\Delta t = t_{n+1} - t_n$, and given state space coordinates $\mathbf{q}_n \in \mathbf{Q}$, $\mathbf{v}_n \in \Re^n$ at t_n. The discretized version of (14) is given by

$$\begin{aligned} \mathbf{q}_{n+1} - \mathbf{q}_n &= \frac{\Delta t}{2}(\mathbf{v}_n + \mathbf{v}_{n+1}) \\ \mathbf{M}(\mathbf{v}_{n+1} - \mathbf{v}_n) &= \Delta t\, \mathbf{f}(\mathbf{q}_n, \mathbf{q}_{n+1}) - \Delta t\, \mathbf{G}(\mathbf{q}_n, \mathbf{q}_{n+1})^T \overline{\boldsymbol{\lambda}} \\ \boldsymbol{\Phi}(\mathbf{q}_{n+1}) &= \mathbf{0} \end{aligned} \tag{18}$$

with

$$\mathbf{f}(\mathbf{q}_n, \mathbf{q}_{n+1}) = \mathbf{Q}(\mathbf{q}_n, \mathbf{q}_{n+1}) - \overline{\nabla} V(\mathbf{q}_n, \mathbf{q}_{n+1}) \tag{19}$$

In the sequel, the algorithm (18) will be called the basic energy-momentum (**BEM**) scheme [3].

The advantageous algorithmic conservation properties of the **BEM** scheme are linked to the notion of a discrete gradient (or derivative) of a function $f : \Re^n \longrightarrow \Re$. In the present work $\overline{\nabla} f(\mathbf{q}_n, \mathbf{q}_{n+1})$ denotes the discrete gradient of *f*. If *f* is at most quadratic then the discrete gradient coincides with the standard gradient evaluated in the mid-point configuration $\mathbf{q}_{n+1/2} = (\mathbf{q}_n + \mathbf{q}_{n+1})/2$, that is, in this case $\overline{\nabla} f(\mathbf{q}_n, \mathbf{q}_{n+1}) = \nabla f(\mathbf{q}_{n+1/2})$. We refer to [1, 3] for further details of the implementation.

3.3 Rotationless formulation of the rigid body

The configuration of a rigid body in three-dimensional Euclidean space can be characterized by the placement of its center of mass $\boldsymbol{\varphi}(t) \in \Re^3$ and a right-handed body frame $\{\mathbf{d}_I\}$, $\mathbf{d}_I \in \Re^3$ (*I*=1,2,3), which specifies the orientation of the body (Fig. 3.3). The vectors $\mathbf{d}_I$ will be occasionally called directors. Let $\mathbf{X} = X_i \mathbf{e}_i$ [2] be a material point which belongs to the reference configuration $V \subset \Re^3$ of the rigid body. The spatial position of $\mathbf{X} \in V$ at time *t* relative to an inertial Cartesian basis $\{\mathbf{e}_I\}$ can now be characterized by

$$\mathbf{x}(\mathbf{X}, t) = \boldsymbol{\varphi}(t) + X_i \mathbf{d}_i(t) \tag{20}$$

Obviously, the configuration of the rigid body can be characterized by the following vector of redundant coordinates (*n*=12):

$$\mathbf{q} = \left[\boldsymbol{\varphi}^T \;\; \mathbf{d}_1^T \;\; \mathbf{d}_2^T \;\; \mathbf{d}_3^T \;\; \mathbf{d}_1^T \right]^T \tag{21}$$

Due to the assumption of rigidity the body frame has to stay orthonormal for all times. Thus there are

[2] In this work the summation convention applies to repeated lower case Roman indices.

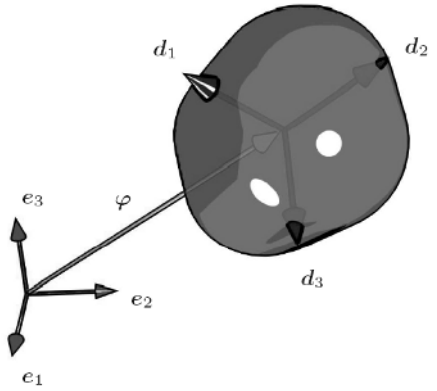

Fig. 5. Spatial rigid body.

m=6 independent internal constraints with associated constraint functions

$$\Phi_{\text{int}}(\mathbf{q})=\begin{bmatrix}\frac{1}{2}\left[\mathbf{d}_1{}^T\mathbf{d}_1-1\right]\\ \frac{1}{2}\left[\mathbf{d}_2{}^T\mathbf{d}_2-1\right]\\ \frac{1}{2}\left[\mathbf{d}_3{}^T\mathbf{d}_3-1\right]\\ \mathbf{d}_1{}^T\mathbf{d}_2\\ \mathbf{d}_1{}^T\mathbf{d}_3\\ \mathbf{d}_2{}^T\mathbf{d}_3\end{bmatrix} \tag{22}$$

The internal constraints given thus rise to the corresponding 6x12 constraint Jacobian

$$\mathbf{G}_{\text{int}}(\mathbf{q})=\begin{bmatrix}\mathbf{0}^T & \mathbf{d}_1{}^T & \mathbf{0}^T & \mathbf{0}^T\\ \mathbf{0}^T & \mathbf{0}^T & \mathbf{d}_2{}^T & \mathbf{0}^T\\ \mathbf{0}^T & \mathbf{0}^T & \mathbf{0}^T & \mathbf{d}_3{}^T\\ \mathbf{0}^T & \mathbf{d}_2{}^T & \mathbf{d}_1{}^T & \mathbf{0}^T\\ \mathbf{0}^T & \mathbf{d}_3{}^T & \mathbf{0}^T & \mathbf{d}_1{}^T\\ \mathbf{0}^T & \mathbf{0}^T & \mathbf{d}_3{}^T & \mathbf{d}_2{}^T\end{bmatrix} \tag{23}$$

Moreover, the kinetic energy expression (22) leads to the constant mass matrix

$$\mathbf{M}=\begin{bmatrix}M_\varphi\mathbf{I} & \mathbf{0} & \mathbf{0} & \mathbf{0}\\ \mathbf{0} & E_1\mathbf{I} & \mathbf{0} & \mathbf{0}\\ \mathbf{0} & \mathbf{0} & E_2\mathbf{I} & \mathbf{0}\\ \mathbf{0} & \mathbf{0} & \mathbf{0} & E_3\mathbf{I}\end{bmatrix} \tag{24}$$

where $\mathbf{I}$ and $\mathbf{0}$ are the 3x3 identity and zero matrices. The equations of motion of the constrained system at hand can now be written in the form of the DAEs (14).

3.4 Incorporation of joint friction

So far the formulations presented above hold for conservative systems with holonomic, scleronomic constraints. Our intention now is to incorporate joint friction, using the coordinate augmentation technique [3, 8]. This technique incorporates rotational degrees of freedom into our rotationless formulation. This enables us to apply torques directly on specific angles. This idea is also the cornerstone of the incorporation of joint friction. We can consider joint friction as a joint torque which is acting against the direction of rotation, proportional to the relative joint velocity.

The incorporation into the continuous set of equations of motion according to (14) can be performed as follows: $\boldsymbol{\tau}_D$

$$\begin{aligned}\dot{\mathbf{q}}-\mathbf{v}&=\mathbf{0}\\ \mathbf{M}\dot{\mathbf{v}}-\mathbf{f}(\mathbf{q})+\mathbf{G}^T(\mathbf{q})\boldsymbol{\lambda}+\boldsymbol{\tau}_D&=\mathbf{0}\\ \boldsymbol{\Phi}(\mathbf{q})&=\mathbf{0}\end{aligned} \tag{25}$$

$\boldsymbol{\tau}_D$ can be viewed as an external torque acting on the system. Here we will model the torque velocity dependent, acting on the augmented coordinates (θ_i), so generally we obtain

$$\boldsymbol{\tau}(\dot{\boldsymbol{\theta}})=d\,\dot{\boldsymbol{\theta}} \tag{26}$$

where d represents the damping coefficient.

A discrete version in an energy consistent setting can be obtained according to the BEM-scheme:

$$\begin{aligned}\mathbf{q}_{n+1}-\mathbf{q}_n&=\frac{\Delta t}{2}(\mathbf{v}_n+\mathbf{v}_{n+1})\\ \mathbf{M}(\mathbf{v}_{n+1}-\mathbf{v}_n)&=\Delta t\,\mathbf{f}(\mathbf{q}_n,\mathbf{q}_{n+1})-\Delta t\,\mathbf{G}(\mathbf{q}_n,\mathbf{q}_{n+1})^T\bar{\boldsymbol{\lambda}}\\ &\quad+\Delta t\boldsymbol{\tau}(\dot{\boldsymbol{\theta}}_{n+1/2})\\ \boldsymbol{\Phi}(\mathbf{q}_{n+1})&=\mathbf{0}\end{aligned} \tag{27}$$

4. 3bar linkage

The numerical example will deal with an underactuated control problem of a three bar linkage. We will demonstrate how friction affects the necessary driving torques in order to prescribe the desired movement.

The three bar linkage represents an open loop chain. As a motivation one can think of a serial robot consisting of three arms. Especially in robotic applica-

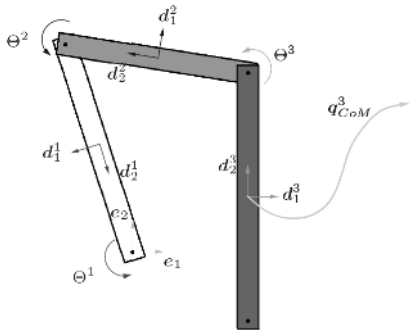

Fig. 6. Schematics for the 3bar linkage.

tions if one is interested in obtaining required driving torques for position problems (control problems), friction effects play a crucial role [9], since an exact modelling of joint friction affects the results dramatically. The purpose within this section is to give a short preview of how to implement joint friction to more complex multibody systems, without emphasizing the exact modelling of friction phenomena. Therefore, we keep the relationship that the friction torques depend linearly on the relative joint velocity (Eq. (26)). What we like to point out is to show how different the results for control problems might become when we implement dissipative effects to a multibody system within an energy-consistent framework.

4.1 Incorporation of control constraints

$$\begin{aligned} \dot{\mathbf{q}} &= \mathbf{0} \\ \mathbf{M}\dot{\mathbf{v}} + \nabla V(\mathbf{q}) + \mathbf{G}(\mathbf{q})^T \boldsymbol{\lambda} + \boldsymbol{\tau}_D + \mathbf{B}(\mathbf{q})^T \overline{\mathbf{m}} &= \mathbf{0} \\ \boldsymbol{\Phi}_{scl/add}(\mathbf{q}) &= \mathbf{0} \\ \boldsymbol{\Phi}_{control}(\mathbf{q},t) &= \mathbf{0} \end{aligned} \tag{28}$$

where usually the control constraints consist of a scleronomic and a rheonomic part

$$\boldsymbol{\Phi}_{control}(\mathbf{q},t) = \underbrace{\sum(\mathbf{q})}_{\text{scleronomic}} + \underbrace{\boldsymbol{\Psi}(t)}_{\text{rheonomic}} \tag{29}$$

The discretization can be accomplished as usual, by using the mid-point evaluation:

$$\begin{aligned} \mathbf{q}_{n+1} - \mathbf{q}_n &= \frac{\Delta t}{2}(\mathbf{v}_n + \mathbf{v}_{n+1}) \\ \mathbf{M}(\mathbf{v}_n + \mathbf{v}_{n+1}) &= \Delta t\, \mathbf{f}(\mathbf{q}_n, \mathbf{q}_{n+1}) - \Delta t\, \mathbf{G}(\mathbf{q}_n, \mathbf{q}_{n+1})^T \overline{\boldsymbol{\lambda}} \\ &\quad + \Delta t\, \boldsymbol{\tau}(\dot{\boldsymbol{\theta}}_{n+1/2}) + \Delta t\, \mathbf{B}^T(\mathbf{q}_n, \mathbf{q}_{n+1}) \overline{\mathbf{m}} \\ \boldsymbol{\Phi}(\mathbf{q}_{n+1}) &= \mathbf{0} \\ \boldsymbol{\Phi}_{control}(\mathbf{q}_{n+1}, t_{n+1}) &= \mathbf{0} \end{aligned} \tag{30}$$

4.2 Rotationless formulation

As obvious from Fig. 13, the present system consists of three rigid linkages, leading to the following configurational vector:

$$\mathbf{q}_{\text{ori}} = \begin{bmatrix} \mathbf{q}^1 \\ \mathbf{q}^2 \\ \mathbf{q}^3 \end{bmatrix} \text{ with } \begin{bmatrix} \boldsymbol{\varphi}^I \\ \mathbf{d}_1^{\,I} \\ \mathbf{d}_2^{\,I} \end{bmatrix} \text{ where } I = 1, 2, 3 \tag{31}$$

All necessary constraints, concerning internal assumptions of rigidity and also external joints, shall not be presented in a detailed fashion. For all who might be interested, standard kinematic pairs are presented in [2]. We now want to summarize the number of redundant coordinates and the number of total constraints, leading to the number of DOF the system at hand has. As obvious from Eq. (31), we have n=18 redundant coordinates, while having in total three bodies, means to invoke another $m_{\text{int}} = 9$ internal constraints due to the assumption of rigidity. Having again three joints leads to another $m_{\text{ext}} = 6$ external constraints. Therefore, the number of DOF equals $n - m_{\text{int}} - m_{\text{ext}} = 18 - 9 - 6 = 3$.

4.3 Coordinate augmentation

Here the coordinate augmentation for the present example is outlined in more detail, since it is vital for our control purpose and the application of joint friction. First, we want to introduce new redundant coordinates into our framework. These coordinates are of rotational character. Taking a glance at Fig. 13, we see that we want to actuate the system at the joints 1 and 2. This means that we also need to incorporate the relative angles in-between as well as the third angle since all joints will be afflicted with friction:

$$\mathbf{q} = \begin{bmatrix} \mathbf{q}_{\text{ori}} \\ \Theta^1 \\ \Theta^2 \\ \Theta^3 \end{bmatrix} \tag{32}$$

The corresponding constraints yield

$$\Phi^I{}_{\text{aug}}(\mathbf{q}) = \Phi^I{}_{\text{aug}}(\mathbf{q}_{\text{ori}}) + \Phi^I{}_{\text{aug}}(\Theta^I) \quad \text{with I=1,2,3} \tag{33}$$

The first augmented coordinate

$$\Phi^1{}_{\text{aug}}(\mathbf{q}_{\text{ori}}) = \mathbf{d}_2{}^1\mathbf{e}_1 + \mathbf{d}_2{}^1\mathbf{e}_2 \tag{34}$$

$$\Phi^1{}_{\text{aug}}\left(\Theta^1\right)=\sin\Theta^1-\cos\Theta^1 \tag{35}$$

For the second and third augmented coordinate we obtain

$$\Phi^k{}_{\text{aug}}\left(\mathbf{q}_{\text{ori}}\right)=\mathbf{d}_2{}^i\mathbf{d}_1{}^j+\mathbf{d}_2{}^i\mathbf{d}_2{}^j \tag{36}$$

$$\Phi^k{}_{\text{aug}}\left(\Theta^k\right)=\sin\Theta^k-\cos\Theta^k \tag{37}$$

where i=2, 3, j=1, 2 and k=2, 3.

The corresponding constraint Jacobian for all augmented angles yields

$$\mathbf{G}^I{}_{\text{aug}}=\left[\mathbf{G}^I{}_{\text{aug}}\left(\mathbf{q}_{\text{ori}}\right)\quad \mathrm{G}^I{}_{\text{aug}}\left(\Theta^I\right)\right]\ \text{with I=1,2,3} \tag{38}$$

where we can write

$$\begin{aligned}
\mathbf{G}^1{}_{\text{aug}}\left(\mathbf{q}_{\text{ori}}\right)&=\left[\mathbf{0}^T{}_{1\text{x}6}\quad \mathbf{e}^T{}_1+\mathbf{e}^T{}_2\quad \mathbf{0}^T{}_{1\text{x}12}\right]\\
\mathbf{G}^2{}_{\text{aug}}\left(\mathbf{q}_{\text{ori}}\right)&=\left[\mathbf{0}^T{}_{1\text{x}6}\quad \left(\mathbf{d}_2{}^2\right)^T\quad \left(\mathbf{d}_2{}^2\right)^T\right.\\
&\qquad \left.\mathbf{0}^T{}_{1\text{x}6}\quad \left(\mathbf{d}_1{}^1+\mathbf{d}_2{}^1\right)^T\quad \mathbf{0}^T{}_{1\text{x}6}\right]\\
\mathbf{G}^2{}_{\text{aug}}\left(\mathbf{q}_{\text{ori}}\right)&=\left[\mathbf{0}^T{}_{1\text{x}6}\quad \left(\mathbf{d}_2{}^3\right)^T\quad \left(\mathbf{d}_2{}^3\right)^T\right.\\
&\qquad \left.\mathbf{0}^T{}_{1\text{x}6}\quad \left(\mathbf{d}_1{}^2+\mathbf{d}_2{}^2\right)^T\right]
\end{aligned} \tag{39}$$

The constraint Jacobian for the augmented part yields

$$\mathrm{G}^I{}_{\text{aug}}\left(\Theta^k\right)=\cos\Theta^I+\sin\Theta^I \tag{40}$$

As obvious from Eq. (39), all terms are at most quadratic. This means that the discrete version coincides with the mid-point evaluation. While, the discrete version of (40) needs a special evaluation (see [3]) and leads to

$$\mathrm{G}^I{}_{\text{aug}}\left(\Theta^I{}_{n+1},\Theta^I{}_n\right)=\frac{\Phi^I{}_{aug}\left(\Theta^I{}_{n+1}\right)-\Phi^I{}_{aug}\left(\Theta^I{}_n\right)}{\Theta^I{}_{n+1}-\Theta^I{}_n} \tag{41}$$

The current intention is to perform an underactuated control of the present 3bar linkage. Therefore, we prescribe the motion of the center of mass (CoM) of the third link. This point follows a linear trajectory, resulting in the control constraint

$$\mathbf{\Phi}_C\left(\mathbf{q},t\right)=\mathbf{q}^3{}_{\text{CoM}}-\mathbf{s}\left(t\right) \tag{42}$$

while $\mathbf{s}(t)$ is characterized by a 9th order polynomial proposed by [4] and which has the following form:

$$\mathbf{s}\left(t\right)=\mathbf{s}_0+\left(126t^5-420t^6+540t^7-315t^8+70t^9\right)\cdot\left(\mathbf{s}_f-\mathbf{s}_0\right) \tag{43}$$

Where $\mathbf{s}_0$ and $\mathbf{s}_f$ mark the initial and final position of the CoM. The time in-between both positions is marked as $t_n=t_2-t_1$.

The application of the **BEM** scheme for control problems needs a corresponding constraint Jacobian for the control constraints to be stated. In this example, since we need two joint torques to be actuated, we obtain

$$\mathbf{B}=\left[\mathbf{0}_{2\text{x}18}\quad \mathbf{I}_{2\text{x}2}\right] \tag{44}$$

4.4 Numerical example

The geometric properties for our example are summarized in Table 1.

The initial position can be specified by the three generalized coordinates

$$\Theta_1=\frac{11}{10}\pi\ ,\quad \Theta_2=\frac{9}{20}\pi\quad \text{and}\quad \Theta_3=0 \tag{45}$$

while the initial velocity is set to $\mathbf{v}=\mathbf{0}$. As described above, we want to solve a control position problem. Starting from point $\mathbf{s}_0$, going to $\mathbf{s}_f$, which are

Table 1. Inertial and geometric properties pertaining to the three legs of the linkage.

body	M	E_1	E_2	length	width
1	30	1.225	143.3	7.57	0.7
2	25	1.02	88.02	6.5	0.7
3	20	1.02	120.42	8.5	0.7

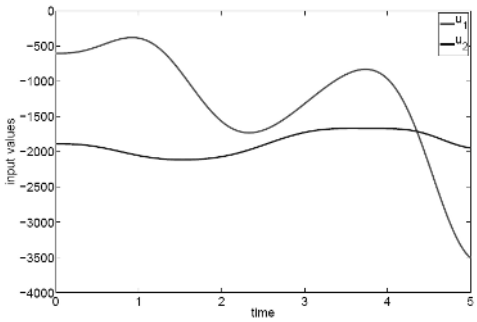

Fig. 7. Inputs for the undamped case.

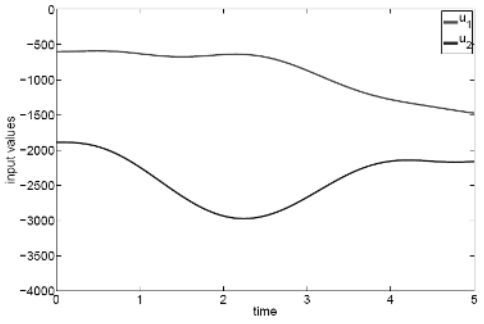

Fig. 8. Inputs for damped case.

specified by

$$\mathbf{s}_0 = \begin{bmatrix} 3.74 \\ 1.79 \end{bmatrix}, \quad \mathbf{s}_f = \begin{bmatrix} 6 \\ 5 \end{bmatrix} \tag{46}$$

We perform two simulations, one without activated friction in the joints and a second one with joint friction. The intention is to show the influence on the inputs (driving torques) and the final position of all links, the step size is chosen to $\Delta t = 0.02$

For activated joint friction, we choose a damping constant of d=3000. The results of the simulation are displayed below. Figs. 7 and 8 give a comparison of the conservative and non-conservative case, showing the necessity of an adequate modelling of joint friction.

5. Conclusions

The present work illustrates the incorporation of dissipation into an energy consistent scheme for multibody dynamics. Starting with the ad hoc approach we incorporated linear viscous friction, where we showed how dissipation could be time integrated properly in order to obtain an energy consistent integration even for non-conservative systems. The extension to multibody systems, could be performed straightforwardly. Here we made use of the coordinate augmentation technique which facilitates the incorporation of joint friction. The modelling was done by applying a joint torque which is acting against the direction of rotation, while the friction model was retained. As an application we presented the underactuated control of a three bar planar manipulator. This showed the relevance of modelling joint friction appropriately, since these effects automatically affect the input values as well as the end-configuration of a control problem, especially for underactuated systems.

Future work will deal with more adequate friction modells; one could also think of a modelling similar to visco elastic material behavior in continuum mechanics.

Acknowledgment

Support for this research was provided by the Deutsche Forschungsgemeinschaft (DFG) under Grant BE 2285/4-2. This support is gratefully acknowledged

References

[1] P. Betsch, The discrete null space method for. The discrete null space method for the energy consistent integration of constrained mechanical systems. Part I: Holonomic constraints. *Comput. Methods Appl. Mech. Engrg.*, 194(50-52) (2005) 5159-5190.

[2] P. Betsch and S. Leyendecker, The discrete null space method for the energy consistent integration of constrained mechanical systems. Part II: Multibody dynamics. *Int. J. Numer. Methods Eng.*, 67(4) (2006) 499-552.

[3] P. Betsch and S. Uhlar. Energy-momentum conserving integration of multibody dynamics. *Multibody System Dynamics*, 17(4) (2007) 243-289.

[4] W. Blajer and K. Kolodziejczyk. A geometric approach to solving problems of control constraints: Theory and a DAE framework. *Multibody System Dynamics*, 11(4) (2004) 343-364.

[5] C. Kane, J. E. Marsden, M. Ortiz and M. West, Variational integrators and the newmark algorithm for conservative and dissipative mechanical systems. *Int. J. Numer. Methods Eng.*, 49 (2000) 1295-1325.

[6] P. Kunkel and V. Mehrmann, *Differential-Algebraic Equations*. European Mathematical Society, (2006).

[7] R. M. Rosenberg, *Analytical dynamics of discrete systems*. Plenum Press, (1977).

[8] S. Uhlar and P. Betsch, On the rotationless formulation of multibody dynamics and its conserving numerical integration. In *Proceedings of ECCOMAS Thematic Conference on Multibody Dynamics*, Politecnico di Milano, Milano, Italy, June 25-28 (2007).

[9] R. Waiboer, R. Aarts and B. Jonker, Velocity dependence of joint friction in robotic manipulators with gear transmissions. In J. M. Goicolea, J.-Cuadrado, and J.C. Garcia~Orden, editors, *Proceed-*

ings of ECCOMAS Thematic Conference on Advances in Computational Multibody Dynamics (CD-ROM), Madrid, Spain, June 21-24 (2005).

Peter Betsch received his Diploma degree in aerospace engineering from the University of Stuttgart, Germany in 1991, the Ph.D. degree in computational mechanics from the University of Hanover, Germany in 1996 and the venia legendi (Habilitation) in mechanics from the University of Kaiserlautern, Germany in 2002. Since 2003 he has been Professor of Computational Mechanics with the University of Siegen, Germany.

Stefan Uhlar received his Diploma degree in mechanical engineering from the University of Kaiserslautern, Germany in 2005. He is a Ph.D. candidate at the chair of computational mechanics at the University of Siegen, Germany.